

# Steady Models of Optically Thin, Magnetically Supported Black Hole Accretion Disks

Hiroshi ODA

*Graduate School of Science and Technology, Chiba University, 1-33 Yayoi-Cho, Inage-ku, Chiba 263-8522*

*oda@astro.s.chiba-u.ac.jp*

Mami MACHIDA

*Division of Theoretical Astronomy, National Astronomical Observatory of Japan, 2-21-1 Osawa, Mitaka, Tokyo 181-8588*

*mami@th.nao.ac.jp*

Kenji E. NAKAMURA

*Department of Sciences, Matsue National College of Technology, 14-4 Nishiikuma-Cho, Matsue, Shimane 690-8518*

*nakamrkn@matsue-ct.jp*

and

Ryoji MATSUMOTO

*Department of Physics, Faculty of Science, Chiba University, 1-33 Yayoi-Cho, Inage-ku, Chiba 263-8522*

*matumoto@astro.s.chiba-u.ac.jp*

(Received ⟨reception date⟩; accepted ⟨acceptance date⟩)

## Abstract

We obtained steady solutions of optically thin, single temperature, magnetized black hole accretion disks assuming thermal bremsstrahlung cooling. Based on the results of 3D MHD simulations of accretion disks, we assumed that the magnetic fields inside the disk are turbulent and dominated by azimuthal component. We decomposed magnetic fields into an azimuthally averaged mean field and fluctuating fields. We also assumed that the azimuthally averaged Maxwell stress is proportional to the total pressure. The radial advection rate of the azimuthal magnetic flux  $\dot{\Phi}$  is prescribed as being proportional to  $\varpi^{-\zeta}$ , where  $\varpi$  is the radial coordinate and  $\zeta$  is a parameter which parameterizes the radial variation of  $\dot{\Phi}$ . We found that when accretion rate  $\dot{M}$  exceeds the threshold for the onset of the thermal instability, a magnetic pressure dominated new branch appears. Thus the thermal equilibrium curve of optically thin disk has a 'Z'-shape in the plane of surface density and temperature. This indicates that as the mass accretion rate increases, a gas pressure dominated optically thin hot accretion disk undergoes a transition to a magnetic pressure dominated, optically thin cool disk. This disk corresponds to the X-ray hard, luminous disk in black hole candidates observed during the transition from a low/hard state to a high/soft state. We also obtained global steady transonic solutions containing such a transition layer.

**Key words:** accretion:accretion disks — black holes — state transition — MHD

## 1. Introduction

Optically thin, hot accretion disks have been studied to explain the X-ray hard state (low/hard state) of black hole candidates. Thorne, Price (1975) proposed that hard X-rays from Cyg X-1 are produced in the inner optically thin hot disks. Shibasaki, Hoshi (1975) studied the structure and stability of optically thin hot accretion disks. Eardley, Lightman, Shapiro (1975) and Shapiro, Lightman, Eardley (1976) constructed a model of optically thin, two temperature accretion disks in which ion temperature is higher than the electron temperature. Ichimaru (1977) pointed out the importance of advection of energy in hot accretion flows and obtained steady models of optically thin disks by equating the radial heat advection  $Q_{\text{adv}}$  and the viscous heating  $Q_{\text{vis}}$ . Such flows, which now are called advection dominated accretion flows (ADAFs) or radiatively inefficient accretion

flows (RIAFs), were studied extensively by Narayan, Yi (1994,1995) and Abramowicz et al. (1995). Abramowicz et al. (1995) obtained local thermal equilibrium curves of optically thin accretion disks by solving  $Q_{\text{vis}} = Q_{\text{adv}} + Q_{\text{rad}}$ , where  $Q_{\text{rad}}$  is the radiative cooling rate. They showed that when the accretion rate exceeds a critical accretion rate, optically thin solution disappears. Above this critical accretion rate, the hard X-ray emitting optically thin hot accretion disk undergoes a transition to an optically thick cool disk which emits soft X-rays. The latter corresponds to the high/soft state (or thermal state) of black hole candidates.

The importance of the magnetic fields on transition between an optically thin hot disk and an optically thick cool disk was discussed by Ichimaru (1977). He suggested that magnetic pressure  $p_{\text{mag}}$  is limited below the gas pressure  $p_{\text{gas}}$  because magnetic flux will escape from the disk by buoyancy. However, the buoyant escape of the

magnetic flux can be suppressed in strongly magnetized disks. Shibata, Tajima, Matsumoto (1990) carried out magnetohydrodynamic (MHD) simulations of the buoyant escape of the magnetic flux due to the Parker instability (Parker 1966) and showed that when the disk is dominated by magnetic pressure, it can stay in low- $\beta$  state ( $\beta = p_{\text{gas}}/p_{\text{mag}} < 1$ ) because the growth rate of the Parker instability is reduced in low- $\beta$  disks due to the magnetic tension. Mineshige, Kusunose, Matsumoto (1995) suggested that low- $\beta$  disk emits hard X-rays. Pariev, Blackman, Boldyrev (2003) obtained steady solutions of optically thick, magnetic pressure dominated disk but they did not consider the optically thin solution including advective cooling. Begelman, Pringle (2006) constructed a model of optically thick low- $\beta$  disk including radiation pressure.

Since magnetic fields contribute both to the angular momentum transport and disk heating, we need to understand how magnetic fields are amplified and maintained in the disk. In conventional theory of accretion disks (e.g., Shakura, Sunyaev 1973), phenomenological  $\alpha$ -viscosity is invoked. However, the physical mechanism which enables angular momentum transport efficient enough to explain the activities of accretion powered sources such as dwarf nova was unknown until Balbus, Hawley (1991) pointed out the importance of the magneto-rotational instability (MRI) in accretion disks. MRI can excite and maintain magnetic turbulence. The Maxwell stress generated by the turbulent magnetic fields efficiently transports angular momentum and enables accretion of the disk material. The growth and the saturation of MRI has been studied by local three-dimensional MHD simulations (e.g., Hawley et al. 1995, 1996; Matsumoto, Tajima 1995; Brandenburg et al. 1995; Sano, Inutuska 2001; Sano et al. 2004) and by global three-dimensional MHD simulations (e.g., Matsumoto 1999; Hawley 2000; Machida et al. 2000; Hawley, Krolik 2001; Hawley, Krolik 2002; Machida, Matsumoto 2003). These global three-dimensional MHD simulations of radiatively inefficient accretion disks indicate that the amplification of magnetic fields saturates when  $\beta \sim 10$  except in the plunging region of black hole accretion disk and in the disk corona, and that the disk approaches to a quasi-steady state. In this quasi-steady state, the average ratio of the Maxwell stress to gas pressure  $\alpha_{\text{SS}}$ , which corresponds to the  $\alpha$ -parameter in the conventional accretion disk theory (Shakura, Sunyaev 1973), is  $\sim 0.01 - 0.1$  (e.g., Hawley 2000; Hawley, Krolik 2001; Machida, Matsumoto 2003).

RXTE observations of state transitions in galactic black hole candidates revealed that some black hole candidates (e.g., GX339-4, XTE J1550-564, and XTE J1859+226) stay in X-ray hard states even when their luminosities exceed 20% of the Eddington luminosity (e.g., Done, Gierliński 2003; Gierliński, Newton 2006). When  $\alpha \lesssim 0.1$  as indicated by global three-dimensional MHD simulations of black hole accretion flows and the energy conversion efficiency  $\eta_e \sim 0.1$ , their luminosities are higher than the critical luminosity above which optically thin steady hot solutions disappear.

Recently, Machida, Nakamura, Matsumoto (2006) carried out global three-dimensional MHD simulations of black hole accretion disks including optically thin radiative cooling. They started the simulation from a radiatively inefficient torus threaded by weak toroidal magnetic fields. As MRI grows, an optically thin, hot accretion disk is formed by transporting angular momentum efficiently. They found by simulation including thermal bremsstrahlung cooling that when the density of the accretion disk exceeds the critical density, cooling instability takes place in the disk. The disk shrinks in the vertical direction with almost conserving the toroidal magnetic flux. They demonstrated that as the disk shrinks, magnetic pressure exceeds the gas pressure because the magnetic pressure increases due to flux conservation, meanwhile the gas pressure decreases due to cooling. When the magnetic pressure becomes dominant, the disk stops shrinking in the vertical direction because the magnetic pressure supports the disk. They found that the disk evolves toward a quasi-equilibrium cool state. During this transition from hot state to cool state, the disk remains optically thin. They explained this quasi-steady state by equating the magnetic heating rate  $Q^+$  and the radiative cooling rate  $Q_{\text{rad}}$  assuming that the Maxwell stress is proportional to the total pressure and that the azimuthal magnetic flux  $\langle B_\varphi \rangle H$  is conserved during the transition, where  $\langle B_\varphi \rangle$  is the mean azimuthal magnetic field, and  $H$  is the half thickness of the disk.

The purpose of this paper is to answer why hard X-ray emitting optically thin disks exist above the critical luminosity. We show steady solutions of optically thin black hole accretion disks by taking into account the magnetic fields, radiative cooling, and advection of energy and magnetic fields. In section 2, we present basic equations. In section 3, we obtain local thermal equilibrium curves. We present the global steady solutions in section 4. Section 5 is devoted for summary and discussion.

## 2. Models and Assumptions

### 2.1. Basic Equations

We extended the basic equations for one-dimensional steady, optically thin black hole accretion flows (e.g., Kato et al. 1998) by incorporating the magnetic fields. We adopt cylindrical coordinates  $(\varpi, \varphi, z)$ . General relativistic effects are simulated by using the pseudo-Newtonian potential  $\psi = -GM/(r - r_s)$  (Paczynsky, Wiita 1980), where  $G$  is the gravitational constant,  $M$  is the mass of the black hole (we assume  $M = 10M_\odot$  in this paper),  $r = (\varpi^2 + z^2)^{1/2}$ , and  $r_s = 2GM/c^2$  is the Schwarzschild radius.

We start from the resistive MHD equations

$$\frac{\partial \rho}{\partial t} + \nabla \cdot (\rho \mathbf{v}) = 0, \quad (1)$$

$$\rho \left[ \frac{\partial \mathbf{v}}{\partial t} + (\mathbf{v} \cdot \nabla) \mathbf{v} \right] = -\rho \nabla \psi - \nabla p_{\text{gas}} + \frac{\mathbf{j} \times \mathbf{B}}{c}, \quad (2)$$

$$\frac{\partial(\rho\epsilon)}{\partial t} + \nabla \cdot [(\rho\epsilon + p_{\text{gas}})\mathbf{v}] - (\mathbf{v} \cdot \nabla)p_{\text{gas}} = q^+ - q^- , \quad (3)$$

$$\frac{\partial \mathbf{B}}{\partial t} = \nabla \times \left( \mathbf{v} \times \mathbf{B} - \frac{4\pi}{c} \eta \mathbf{j} \right) , \quad (4)$$

where  $\rho$  is the density,  $\mathbf{v}$  is the velocity,  $\mathbf{B}$  is the magnetic field,  $\mathbf{j} = c\nabla \times \mathbf{B}/4\pi$  is the current density,  $p_{\text{gas}} = \mathfrak{R}\rho T/\mu$  is the gas pressure,  $T$  is the temperature,  $\epsilon = 3\mathfrak{R}T/2\mu$  is the internal gas energy,  $\mathfrak{R}$  is the gas constant,  $\mu$  is the mean molecular weight (we assumed to be 0.617),  $q^+$  is the heating rate,  $q^-$  is the radiative cooling rate, and  $\eta$  is the resistivity.

Global three-dimensional MHD simulations (e.g., Matsumoto 1999, Hawley 2000, Machida et al. 2000; Hawley, Krolik 2001, 2002; Machida, Matsumoto 2003; Machida et al. 2004, 2006) showed that in radiatively inefficient accretion disks the amplified turbulent magnetic fields saturates when  $\beta = p_{\text{gas}}/p_{\text{mag}} \sim 10$  except in the plunging region and in the disk corona. Inside the disk, the azimuthal component of magnetic field dominates the poloidal component.

Machida, Nakamura, Matsumoto (2006) carried out three-dimensional MHD simulation of black hole accretion disks including optically thin radiative cooling and showed that when the mass accretion rate exceeds the threshold for the onset of the cooling instability, a magnetically supported disk is formed. The magnetic pressure exceeds the gas pressure because magnetic fields are amplified due to the vertical contraction of the disk, meanwhile the gas pressure decreases due to cooling.

We have to take into account magnetic fields to study the evolution of accretion disks in this regime. We decompose the magnetic fields into the axisymmetric toroidal component (mean field)  $\bar{\mathbf{B}} = \langle B_\varphi \rangle \hat{\mathbf{e}}_\varphi$  and the fluctuating fields  $\delta\mathbf{B} = \delta B_\varpi \hat{\mathbf{e}}_\varpi + \delta B_\varphi \hat{\mathbf{e}}_\varphi + \delta B_z \hat{\mathbf{e}}_z$  and decompose the velocity into the mean velocity  $\bar{\mathbf{v}} = (v_\varpi, v_\varphi, v_z)$  and fluctuating velocity  $\delta\mathbf{v}$ . Here  $\langle \rangle$  denotes the azimuthal average and  $B_\varpi = \delta B_\varpi$ ,  $B_\varphi = \langle B_\varphi \rangle + \delta B_\varphi$ , and  $B_z = \delta B_z$ . We assume that the fluctuating components vanish when azimuthally averaged ( $\langle \delta\mathbf{v} \rangle = \langle \delta\mathbf{B} \rangle = 0$ ). Thus, the azimuthally averaged magnetic field and velocity are  $\langle \mathbf{B} \rangle = \langle B_\varphi \rangle \hat{\mathbf{e}}_\varphi$  and  $\langle \mathbf{v} \rangle = \bar{\mathbf{v}}$ , respectively.

Let us derive azimuthally averaged equations assuming that the disk is in a steady state. We assume that  $|\langle B_\varphi \rangle + \delta B_\varphi| \gg |\delta B_\varpi|, |\delta B_z|$ . By azimuthally averaging equations (1) - (3) and ignoring the second order term of  $\delta B_\varpi$  and  $\delta B_z$ , we obtain

$$\frac{\partial}{\partial \varpi} (\varpi \rho v_\varpi) + \frac{\partial}{\partial z} (\rho v_z) = 0 , \quad (5)$$

$$\rho v_\varpi \frac{\partial v_\varpi}{\partial \varpi} + \rho v_z \frac{\partial v_\varpi}{\partial z} - \frac{\rho v_\varphi^2}{\varpi} = -\rho \frac{\partial \psi}{\partial \varpi} - \frac{\partial p_{\text{tot}}}{\partial \varpi} + \frac{\langle B_\varphi^2 \rangle}{4\pi \varpi} , \quad (6)$$

$$\begin{aligned} \rho v_\varpi \frac{\partial v_\varphi}{\partial \varpi} + \rho v_z \frac{\partial v_\varphi}{\partial z} + \frac{\rho v_\varpi v_\varphi}{\varpi} \\ = \frac{1}{\varpi^2} \frac{\partial}{\partial \varpi} \left[ \varpi^2 \frac{\langle B_\varpi B_\varphi \rangle}{4\pi} \right] + \frac{\partial}{\partial z} \left( \frac{\langle B_\varphi B_z \rangle}{4\pi} \right) , \end{aligned} \quad (7)$$

$$\rho v_\varpi \frac{\partial v_z}{\partial \varpi} + \rho v_z \frac{\partial v_z}{\partial z} = -\frac{\partial \psi}{\partial z} - \frac{1}{\rho} \frac{\partial p_{\text{tot}}}{\partial z} , \quad (8)$$

$$\begin{aligned} \frac{\partial}{\partial \varpi} [(\rho\epsilon + p_{\text{gas}}) v_\varpi] + \frac{v_\varpi}{\varpi} (\rho\epsilon + p_{\text{gas}}) + \frac{\partial}{\partial z} [(\rho\epsilon + p_{\text{gas}}) v_z] \\ - v_\varpi \frac{\partial p_{\text{gas}}}{\partial \varpi} - v_z \frac{\partial p_{\text{gas}}}{\partial z} = q^+ - q^- , \end{aligned} \quad (9)$$

where  $p_{\text{tot}} = p_{\text{gas}} + p_{\text{mag}}$  is the total pressure and  $p_{\text{mag}} = \langle B_\varphi^2 \rangle / 8\pi$  is the azimuthally averaged magnetic pressure.

Global three-dimensional MHD simulations showed that, in radiatively inefficient disks, azimuthally averaged total stress inside the disk is dominated by the  $\varpi\varphi$ -component of the Maxwell stress  $\langle t_{\varpi\varphi} \rangle \sim \langle B_\varpi B_\varphi / 4\pi \rangle$  and that the average ratio of the Maxwell stress to the magnetic pressure,  $\alpha_m \equiv -\langle B_\varpi B_\varphi / 4\pi \rangle / \langle p_{\text{mag}} \rangle$ , is nearly constant ( $\sim 0.2 - 0.5$ ; e.g., Hawley, Krolik 2001, 2002; Pessah et al. 2006). Since  $\beta \sim 10$  inside the disk except in the plunging region,  $\alpha_B \equiv -\langle B_\varpi B_\varphi / 4\pi \rangle / p_{\text{tot}} \sim 0.01 - 0.1$  (e.g., Hawley, Krolik 2001). Machida, Nakamura, Matsumoto (2006) showed that  $\alpha_B \sim 0.05 - 0.1$  in cooling dominated magnetic pressure supported disk. According to their numerical results, we assume that the azimuthally averaged  $\varpi\varphi$ -component of the Maxwell stress is proportional to the total pressure ( $\langle B_\varpi B_\varphi / 4\pi \rangle = -\alpha_B p_{\text{tot}}$ ). Thus, equation (7) becomes

$$\begin{aligned} \rho v_\varpi \frac{\partial v_\varphi}{\partial \varpi} + \rho v_z \frac{\partial v_\varphi}{\partial z} + \frac{\rho v_\varpi v_\varphi}{\varpi} \\ = \frac{1}{\varpi^2} \frac{\partial}{\partial \varpi} [\varpi^2 (-\alpha_B p_{\text{tot}})] + \frac{\partial}{\partial z} \left( \frac{\langle B_\varphi B_z \rangle}{4\pi} \right) . \end{aligned} \quad (10)$$

We note that in the turbulent accretion disk, the average of the radial component of magnetic fields,  $\langle B_\varpi \rangle$ , is small because positive and negative  $B_\varpi$  cancel out. On the other hand, the product of the radial and the toroidal components,  $B_\varpi B_\varphi$ , does not change sign in the non-linear state (see figure 1). Thus, we can not neglect  $\langle B_\varpi B_\varphi \rangle$  term.

## 2.2. Heating and Cooling Rates

The other key factor is the heating rate expressed as  $q_{\text{vis}}^+ = t_{\varpi\varphi} \varpi (d\Omega/d\varpi)$  in conventional theory, where  $\Omega$  is the angular velocity. Meanwhile, three-dimensional MHD simulations indicate that the total dissipative heating rate (a major part of dissipation is due to the thermalization of magnetic energy via magnetic reconnection) is  $q^+ \sim \langle B_\varpi B_\varphi / 4\pi \rangle \varpi (d\Omega/d\varpi)$  and that this dissipation occurs throughout the disk (e.g., Hirose et al. 2006).

We assume the magnetic heating as the heating mechanism in the disk and set the heating term as follows:

$$q^+ = \frac{\langle B_\varpi B_\varphi \rangle}{4\pi} \varpi \frac{d\Omega}{d\varpi} = -\alpha_B p_{\text{tot}} \varpi \frac{d\Omega}{d\varpi} . \quad (11)$$

As the cooling mechanism, we assume the radiative cooling by the optically thin thermal bremsstrahlung emission. Hence, the cooling rate is expressed as,

$$q^- = 6.2 \times 10^{20} \rho^2 T^{1/2} \text{ ergs s}^{-1} \text{ cm}^{-3} . \quad (12)$$

### 2.3. Vertically Integrated Equations

We assume that the temperature  $T$ ,  $\beta (= p_{\text{gas}}/p_{\text{mag}})$ , radial velocity  $v_{\varpi}$ , and specific angular momentum  $\ell (= \varpi v_{\varphi})$  are independent of  $z$ . Machida et al. (2000) and Miller, Stone (2000) showed that the magnetic loops emerge from the disk and form coronal magnetic loops. In this paper, we focus on the disk and ignored the low density and low  $\beta$  corona. We assume hydrostatic balance in the vertical direction and therefore ignore the left-hand side of the  $z$ -component of momentum equation. Under these assumptions, the surface density  $\Sigma$ , the vertically integrated pressure  $W$ , and the half thickness of the disk  $H$  are given by

$$\Sigma = \int_{-\infty}^{\infty} \rho dz = \sqrt{2\pi} \rho_0(\varpi) H, \quad (13)$$

$$W = \int_{-\infty}^{\infty} p_{\text{tot}} dz = \frac{\Re T}{\mu} (1 + \beta^{-1}) \Sigma, \quad (14)$$

$$H = \frac{1}{\Omega_K} \left( \frac{W}{\Sigma} \right)^{1/2} = \frac{1}{\Omega_K} \left[ \frac{\Re T}{\mu} (1 + \beta^{-1}) \right]^{1/2}, \quad (15)$$

where  $\rho_0(\varpi)$  is the equatorial density and  $\Omega_K = (GM/\varpi)^{1/2}/(\varpi - r_s)$  is the Keplerian angular speed.

We now integrate other basic equations in the vertical direction. Since the density vanishes at the disk surface, the vertically integrated equation of continuity is expressed as

$$\dot{M} = -2\pi\varpi\Sigma v_{\varpi}, \quad (16)$$

where  $\dot{M}$  is the accretion rate.

The  $\varpi$ -component of the vertically integrated momentum equation can be obtained by using  $\langle B_{\varphi}^2 \rangle = 8\pi p_{\text{gas}}\beta^{-1} = 8\pi\beta^{-1}p_{\text{tot}}/(1 + \beta^{-1})$ ,

$$v_{\varpi} \frac{dv_{\varpi}}{d\varpi} + \frac{1}{\Sigma} \frac{dW}{d\varpi} = \frac{\ell^2 - \ell_K^2}{\varpi^3} - \frac{W}{\Sigma} \frac{d\ln\Omega_K}{d\varpi} - \frac{2}{\varpi} \frac{\beta^{-1}}{1 + \beta^{-1}} \frac{W}{\Sigma}, \quad (17)$$

where  $\ell_K = \varpi^2\Omega_K$  is the Keplerian angular momentum and the second term on the right-hand side is a correction resulting from the fact that the radial component of the gravitational force changes with height ( see Matsumoto et al. 1984).

Assuming that the last term of the  $\varphi$ -component of momentum equation vanishes at the disk surface, the  $\varphi$ -component of vertically integrated momentum equation is

$$\dot{M}(\ell - \ell_{\text{in}}) = 2\pi\alpha_B\varpi^2 W, \quad (18)$$

where  $\ell_{\text{in}}$  is the specific angular momentum swallowed by the black hole.

The vertically integrated energy equation is

$$Q_{\text{adv}} = Q^+ - Q^-, \quad (19)$$

where

$$Q_{\text{adv}} = \frac{\dot{M}}{2\pi\varpi^2} \frac{\Re T}{\mu} \xi \quad (20)$$

is the advective cooling rate, where

$$\xi = -\frac{3}{2} \frac{d\ln T}{d\ln\varpi} + \frac{d\ln\Sigma}{d\ln\varpi} - \frac{d\ln H}{d\ln\varpi}, \quad (21)$$

and

$$Q^+ = \int_{-\infty}^{\infty} q^+ dz = -\alpha_B W \varpi \frac{d\Omega}{d\varpi}, \quad (22)$$

$$Q^- = \int_{-\infty}^{\infty} q^- dz = 6.2 \times 10^{20} \rho_0^2 T^{1/2} \sqrt{\pi} H \quad (23)$$

are the heating and cooling rates integrated in the vertical direction.

### 2.4. Prescription of the Advection Rate of the Toroidal Magnetic Flux

The basic equations of the steady, magnetized accretion disks can be closed by specifying the radial distribution of magnetic field. By azimuthally averaging equation (4), we obtain

$$\frac{\partial \langle B_{\varphi} \rangle \hat{\mathbf{e}}_{\varphi}}{\partial t} = \nabla \times (\bar{\mathbf{v}} \times \langle B_{\varphi} \rangle \hat{\mathbf{e}}_{\varphi}) + \nabla \times (\delta \mathbf{v} \times \delta \mathbf{B}) + \nabla \times (\eta \nabla \times \langle B_{\varphi} \rangle \hat{\mathbf{e}}_{\varphi}), \quad (24)$$

where the second term on the right-hand side is the dynamo term and the last term is the magnetic diffusion term. If we neglect these terms and assume that the disk is in a steady state, we have

$$0 = -\frac{\partial}{\partial z} (v_z \langle B_{\varphi} \rangle) - \frac{\partial}{\partial \varpi} (v_{\varpi} \langle B_{\varphi} \rangle). \quad (25)$$

Assuming that the azimuthally averaged toroidal magnetic fields vanish at the disk surface, we can integrate equation (25) in the vertical direction and obtain,

$$\dot{\Phi} \equiv \int_{-\infty}^{\infty} v_{\varpi} \langle B_{\varphi} \rangle dz = \text{constant}. \quad (26)$$

The radial advection rate of the toroidal magnetic flux  $\dot{\Phi}$  (hereafter we call it flux advection rate) can be evaluated by completing the vertical integration as

$$\dot{\Phi} = -v_{\varpi} B_0(\varpi) \sqrt{4\pi} H, \quad (27)$$

where

$$\begin{aligned} B_0(\varpi) &= \langle B_{\varphi} \rangle(\varpi; z=0) \\ &= 2^{5/4} \pi^{1/4} (\Re T / \mu)^{1/2} \Sigma^{1/2} H^{-1/2} \beta^{-1/2} \end{aligned} \quad (28)$$

is the azimuthally averaged equatorial toroidal magnetic field. In accretion disks,  $\dot{\Phi}$  is not always conserved because  $\dot{\Phi}$  can change with radius by the presence of the dynamo term and the magnetic diffusion term in equation (24). According to Machida, Nakamura, Matsumoto (2006),  $\dot{\Phi} \propto \varpi^{-1}$  in the quasi steady state. Based on this simulation result, we parametrize the dependence of  $\dot{\Phi}$  on  $\varpi$  by introducing a parameter  $\zeta$  as

$$\dot{\Phi}(\varpi; \zeta, \dot{M}) \equiv \dot{\Phi}_{\text{out}}(\dot{M}) \left( \frac{\varpi}{\varpi_{\text{out}}} \right)^{-\zeta}, \quad (29)$$

where  $\dot{\Phi}_{\text{out}}$  is the flux advection rate at the outer boundary  $\varpi = \varpi_{\text{out}}$ . When  $\zeta = 0$ , the magnetic flux is conserved. When  $\zeta > 0$ , the magnetic flux increases with approaching to the black hole.

### 3. Local Model

#### 3.1. Local Approximation of Energy Equation

Before obtaining global transonic solutions, we solve the energy equation  $Q^+ = Q_{\text{adv}} + Q^-$  locally at some specified radius to obtain thermal equilibrium curves of optically thin black hole accretion flows.

We approximated the energy equation in order to be solved locally. We evaluated  $\xi$  by using results of global three-dimensional MHD simulations of black hole accretion flows. According to the results by Machida et al. (2004),  $T \propto \varpi^{-1}$ ,  $\Sigma \propto \varpi^{1/2}$ , and  $H \propto \varpi$ , thus  $\xi = 1$ . Furthermore, we assume  $\Omega = \Omega_K$ . In our local model, we adopt  $\ell_{\text{in}} = \ell_K(3r_s) = 1.8371$ ,  $\varpi = 5r_s$  and  $\alpha_B = 0.05$  as the fiducial value, hence, the free parameters are now  $\dot{M}$  and  $\zeta$ .

The flux advection rate  $\dot{\Phi}$  is determined from equation (29) by specifying  $\dot{\Phi}_{\text{out}}$ . We assume that at  $\varpi = \varpi_{\text{out}} = 1000r_s$ ,  $\ell_{\text{out}} = \ell_K$ ,  $T_{\text{out}} = T_{\text{virial}}$  and  $\beta_{\text{out}} = 10$ , where  $T_{\text{virial}} = (\mu c^2/3\mathfrak{R})(\varpi_{\text{out}}/r_s)^{-1}$  is the virial temperature at  $\varpi = \varpi_{\text{out}}$ . Since we fixed  $T$ ,  $\beta$ , and  $\ell$  at  $\varpi = \varpi_{\text{out}}$ , equations (14), (15) and (18) indicate that  $W_{\text{out}} \propto \Sigma_{\text{out}}$ ,  $H_{\text{out}} \sim \text{constant}$  and  $W_{\text{out}} \propto \dot{M}$ , respectively. We find  $\Sigma_{\text{out}} \propto \dot{M}$ , thus, equation (16) indicates that  $v_{\varpi_{\text{out}}} \sim \text{constant}$ . Therefore, equation (28) gives  $B_0(\varpi_{\text{out}}) \propto \Sigma_{\text{out}}^{1/2} \propto \dot{M}^{1/2}$  and equation (27) gives  $\dot{\Phi}_{\text{out}} \propto \dot{M}^{1/2}$ .

#### 3.2. Numerical Results

In figure 2, we show the thermal equilibrium curves at  $\varpi = 5r_s$  for optically thin accretion disks. The equilibrium curves are plotted on the  $\Sigma - \dot{M}$ ,  $\Sigma - T$ ,  $\Sigma - \beta$  and  $\Sigma - \tau_{\text{eff}}$  plane for  $\zeta = 0$ , 0.4 and 0.8. In the top panel of figure 2,  $\dot{M}$  is normalized by the Eddington accretion rate  $M_{\text{Edd}} = 4\pi GM/(\eta_e \kappa_{\text{esc}} c) = 1.64 \times 10^{19} (0.1/\eta_e) (M/10M_{\odot}) \text{ g s}^{-1}$ , where the energy conversion efficiency  $\eta_e$  and the electron scattering opacity  $\kappa_{\text{esc}}$  are taken to be  $\eta_e = 0.1$  and  $\kappa_{\text{esc}} = 0.34 \text{ cm}^2 \text{ g}^{-1}$ , respectively. The equilibrium curves consist of three branches; (1) gas pressure supported, advectively cooled branch, which is thermally stable, i.e. ADAF branch, (2) gas pressure supported, radiatively cooled branch, which is thermally unstable (SLE branch obtained by Shapiro, Lightman, Eardley 1976), and (3) magnetic pressure supported, radiatively cooled branch, which is thermally stable. We call the last branch “low- $\beta$  branch”. We find that the low- $\beta$  branch exists even when  $\dot{M} \gtrsim 0.1M_{\text{Edd}}$ , which corresponds to  $L \gtrsim 0.1L_{\text{Edd}}$ .

It may be worth noting that on the low- $\beta$  branch,  $\dot{M} \propto \Sigma$  and  $T \propto \Sigma^{-2}$ . This dependence can be explained as follows. When the magnetic pressure is dominant,  $W \sim B_0^2 H \propto (v_{\varpi} B_0 H)^2 / (v_{\varpi}^2 H) \propto \dot{\Phi}^2 / (v_{\varpi}^2 H) \propto \dot{M} / (v_{\varpi}^2 H)$ . We find  $v_{\varpi} \propto H^{-1/2}$  because equation (18) gives  $W \propto \dot{M}$ . Since equation (15) gives  $H \propto (W/\Sigma)^{1/2} \propto (\dot{M}/\Sigma)^{1/2}$

and equation (16) gives  $v_{\varpi} \propto \dot{M}/\Sigma$ , we obtain  $\dot{M} \propto \Sigma$  and  $H \sim \text{constant}$ . When the heating balances with the radiative cooling ( $Q^+ = Q^-$ ), since  $Q^+ \propto W$  and  $Q^- \propto \Sigma^2 T^{1/2} / H$ , we find  $W \propto \dot{M} \propto \Sigma^2 T^{1/2} / H$ . Using  $\dot{M} \propto \Sigma$  and  $H \sim \text{constant}$ , we obtain  $T \propto \Sigma^{-2}$ .

The bottom panel of figure 2 shows the effective optical depth  $\tau_{\text{eff}} = \sqrt{\kappa_{\text{esc}} \kappa_{\text{ff}}} \Sigma / 2$  where  $\kappa_{\text{ff}} = 6.4 \times 10^{22} \rho_0(\varpi) T^{-3.5} \text{ cm}^2 \text{ g}^{-1}$  is the opacity of free-free absorption. Note that, when  $\zeta < 0.3$ , the effective optical depth exceeds unity when  $\dot{M} > 0.1M_{\text{Edd}}$ , thus, optically thin approximation is no longer valid. We will extend the low- $\beta$  solution to optically thick regime in subsequent papers.

One may wonder why  $T$  and  $\beta$  increase with  $\zeta$  when  $\Sigma$  is fixed in the low- $\beta$  branch in figure 2. When  $\Sigma$  is fixed, since  $W \sim (B_0/8\pi)H \propto B_0^2 W^{1/2}$  on the low- $\beta$  branch,  $Q^+ \propto W \propto B_0^4$  increases with  $\zeta$ . Thus, the equilibrium temperature increases according to  $W \propto Q^+ = Q^- \propto T^{1/2} / H \propto T^{1/2} / W^{1/2}$  as  $T \propto W^3 \propto Q^+{}^3$ . The plasma  $\beta$  on the low- $\beta$  branch is given by  $\beta \sim \Sigma T / W \propto T^{2/3}$  when  $\Sigma$  is fixed. Thus,  $\beta$  increases with  $\zeta$ .

Figure 3 shows the thermal equilibrium curves for  $\alpha_B = 0.01$ . When  $\alpha_B$  is smaller, the transition from the ADAF branch to the low- $\beta$  branch takes place at smaller  $\Sigma$  because heating rate is smaller. The bottom panel of figure 3 indicates that as the accretion rate increases, the disk becomes optically thick before the mass accretion rate attains  $\dot{M} \sim 0.1M_{\text{Edd}}$  when  $\zeta < 0.5$ .

In figure 4, we show the radial dependence of the  $\dot{M}_{\text{crit}}$  above which the ADAF branch disappears for  $\zeta = 0.4$  and  $\alpha_B = 0.05$  (solid), 0.03 (dashed), and 0.01 (dotted). The critical accretion rate  $\dot{M}_{\text{crit}}$  increases inward. This indicates that as  $\dot{M}$  increases the transition from ADAF branch to low- $\beta$  branch takes place first at large radius and propagates inward.

### 4. Global Model

We numerically solved equations (16)-(19) inward starting from the outer boundary at  $\varpi = \varpi_{\text{out}}$  by specifying  $\ell_{\text{out}}$ ,  $T_{\text{out}}$ ,  $\beta_{\text{out}}$ , and four parameters  $\alpha_B$ ,  $\dot{M}$ ,  $\zeta$ , and  $\ell_{\text{in}}$ . By adjusting the parameter  $\ell_{\text{in}}$ , we obtained a global transonic solution which smoothly passes the sonic point (e.g., Nakamura et al. 1997). The free parameters are now  $\alpha_B$ ,  $\dot{M}$ , and  $\zeta$ . We adopt  $\alpha_B = 0.05$ .

We locate the outer boundary at  $\varpi_{\text{out}} = 1000r_s$ , and imposed the boundary conditions  $\ell_{\text{out}} = 0.45\ell_K$ ,  $T_{\text{out}} = T_{\text{virial}}$  and  $\beta_{\text{out}} = 10$ . We adopt backward-Euler method as an integration method (see Matsumoto et al. 1984).

In figure 5, we show the radial structure of the disks when  $\zeta = 1$  and  $\dot{M}/M_{\text{Edd}} = 0.0002$  (solid), 0.2446 (dashed), 0.3181 (dashed-dotted), and 0.4094 (dotted). When  $\dot{M}$  is small, since  $\Sigma$  is small in the whole disk, the radiative cooling is inefficient. Thus the gas does not cool down. The heating is balanced mainly with the advective cooling. Furthermore, the flow is sub-Keplerian. When  $\dot{M}$  is large, the disk can be divided into four regions; the outer boundary region  $\varpi \gtrsim 400r_s$ , the outer transition region  $400r_s \gtrsim \varpi \gtrsim 150r_s$ , the inner low- $\beta$  region

$150r_s \gtrsim \varpi \gtrsim 50r_s$  and the inner ADAF region  $\varpi \lesssim 50r_s$  when  $\dot{M}/\dot{M}_{\text{Edd}} = 0.3181$ . Near the outer boundary, the accretion flow is advection dominated;  $Q_{\text{adv}} > Q^-$ . However, in the outer transition region, the radiative cooling overcomes the heating as  $\Sigma$  increases. Below this radius  $T$  decreases inward, and  $\beta$  decreases, that is, the magnetic pressure increases inward due to the magnetic flux conservation. At  $\varpi \sim 100r_s$ ,  $T$  ceases to decrease inward because the heating balances with the radiative cooling. In the inner ADAF region, the advective cooling  $Q_{\text{adv}}$  increases as  $T$  increases, and balances with the heating  $Q^+$ . The radiative cooling decreases in the innermost region as  $\Sigma$  decreases.

To check the validity of the optically thin approximation, we show the radial distribution of  $\tau_{\text{eff}}$  in panel (f) of figure 5. In these models,  $\tau_{\text{eff}}$  is less than unity.

In the top panel of figure 6, we plotted the  $\Sigma - \dot{M}$  relation at  $\varpi = 5r_s$  obtained by global transonic solutions. We also computed the luminosity  $L$  by integrating the radiative cooling all over the disk. In the bottom panel of figure 6, we show the dependence of  $L$ , which is normalized by the Eddington luminosity  $L_{\text{Edd}} = \eta_e \dot{M}_{\text{Edd}} c^2 = 1.47 \times 10^{39} (M/10M_\odot) \text{ erg s}^{-1}$ , on the surface density at  $\varpi = 5r_s$ . The optically thin low- $\beta$  solution extends to  $L \sim 0.1 L_{\text{Edd}}$ . Note that when  $\Sigma \sim 10 \text{ g cm}^{-2}$  at  $\varpi \sim 5r_s$  the disk luminosity is only 1% of the Eddington luminosity even though the mass accretion rate attains  $\dot{M} \sim 0.1 \dot{M}_{\text{Edd}}$ . The disk is underluminous because the innermost region of the disk is still advection dominated, that is, radiatively inefficient. The dotted curves in figure 6 ( $\zeta = 0.6$ ) show that when  $10 \text{ g cm}^{-2} < \Sigma < 100 \text{ g cm}^{-2}$ ,  $L$  increases although  $\dot{M}$  is nearly constant. It indicates that the disk luminosity increases as the area of the radiative cooling dominated region increases. The disk luminosity can exceed 10% of the Eddington luminosity only when  $\dot{M} \gtrsim \dot{M}_{\text{Edd}}$ .

## 5. Summary and Discussion

We obtained steady transonic solutions of optically thin black hole accretion flows by including magnetic fields. We theoretically confirmed the simulation result by Machida, Nakamura, Matsumoto (2006) that an optically thin hot disk undergoes a transition to an optically thin magnetic pressure dominated disk when the accretion rate exceeds a threshold. In addition to the ADAF branch and the SLE branch known for optically thin disks, we found a low- $\beta$  branch in which the magnetic heating balances with the radiative cooling.

In section 3, we obtained local solutions for single temperature disks dominated by the toroidal magnetic fields. As a consequence, we obtained three thermal equilibrium branches, ADAF, SLE and low- $\beta$  branches.

Based on the results of global three-dimensional MHD simulations by Machida, Nakamura, Matsumoto (2006), we assumed that the Maxwell stress is proportional to the total pressure,  $\langle B_\varpi B_\varphi / 4\pi \rangle = -\alpha_B p_{\text{tot}}$ . Here  $\alpha_B$  is a parameter corresponding to the  $\alpha$ -parameter in conventional theory of accretion disks. Note that in magnet-

ically dominated disks, since  $p_{\text{tot}} \sim p_{\text{mag}}$ , the Maxwell stress is proportional to the magnetic pressure. In gas pressure dominated disk, since  $\beta \sim 10$  inside the disk except in the plunging region of black hole accretion disks,  $p_{\text{mag}} \sim 0.1 p_{\text{tot}}$ . Thus our assumption is consistent with the results of global three-dimensional MHD simulations by Hawley, Krolik (2001, 2002), in which they showed that Maxwell stress is proportional to magnetic pressure (see also Pessah et al. 2006).

In this paper, we assumed that  $\alpha_B$  does not depend on  $\beta$  and is uniform for simplicity. Let us discuss the dependence of  $\alpha_B$  on the strength of azimuthal magnetic fields. Pessah, Psaltis (2005) studied the stability of accretion disks with superthermal azimuthal fields and showed that MRI is suppressed when the Alfvén speed inside the disk  $v_A$  exceeds the geometrical mean of the sound speed  $c_s$  and the Keplerian rotation speed  $v_K$  (i.e.  $v_A \geq \sqrt{c_s v_K}$ ). Thus, the magnetic turbulence will be suppressed when this criterion is satisfied. In the three-dimensional MHD simulation reported by Machida, Nakamura, Matsumoto (2006), fluctuating magnetic field decreases as  $\beta$  decreases to  $\beta \sim 0.1$  (see Fig. 5b in Machida et al. 2006) because MRI is suppressed. Even in such disks, however, the angular momentum is transported by the Maxwell stress of mean magnetic fields, and  $\alpha_B$  remained  $\alpha_B \sim 0.05 - 0.1$  (Machida, Nakamura, Matsumoto 2006). We need to carry out simulations for longer period to study the dependence of  $\alpha_B$  on  $\beta$ . We should note that  $\alpha_B$  increases in the innermost plunging region of the disk (e.g., Hawley, Krolik 2002; Machida et al. 2004). Thus, this dependence may affect on the global solutions passing through the sonic point in the plunging region. However, its effect will be small for local solutions outside the plunging region. We should also note that we neglected the low- $\beta$  corona above accretion disks. It will be our future work to take into account the effects of such corona and outflows emerging from the disk.

The heating rate inside the disk originates from the thermalization of magnetic energy via the magnetic reconnection and is expressed as  $q^+ = \langle B_\varpi B_\varphi / 4\pi \rangle \varpi (d\Omega/d\varpi) = -\alpha_B p_{\text{tot}} \varpi (d\Omega/d\varpi)$ . This expression is based on the three-dimensional MHD simulations both in gas pressure dominant disks (Hirose et al. 2006) and in magnetic pressure dominant disks (Machida et al. 2006). If MRI is suppressed when  $v_A > \sqrt{c_s v_K}$  as Pessah, Psaltis (2005) suggested, the dissipative heating rate  $Q^+$  may decrease. Therefore, the disk temperature will become smaller than that shown in figure 3.

As we showed in section 3.2,  $\dot{M} \propto \Sigma$  and  $T \propto \Sigma^{-2}$  on the low- $\beta$  branch. However, this dependence is different from that given by Machida, Nakamura, Matsumoto (2006) in which they derived  $\dot{M} \propto \Sigma^{1/3}$  and  $T \propto \Sigma^{-4}$ . This difference comes from the fact that in our model  $\dot{\Phi} \propto v_\varpi B_\vartheta \propto \dot{M}^{1/2}$  (that is, flux advection rate increases as mass accretion rate increases). Meanwhile Machida, Nakamura, Matsumoto (2006) assumed  $BH \sim \text{constant}$ .

The critical accretion rate for the ADAF solution  $\dot{M}_{\text{crit}}$  increases as decreasing the radius when  $\varpi > 10r_s$ , and has a maximum around  $\varpi \sim 10r_s$ . This fact indicates that in

the region  $\varpi > 10r_s$ , the low- $\beta$  region propagates inward as  $\dot{M}$  increases. When  $\dot{M}$  exceeds the maximum of  $\dot{M}_{\text{crit}}$ , whole disk will become low  $\beta$ .

According to our local solutions, optically thin low- $\beta$  branches can exist above the critical accretion rate  $\dot{M}_{\text{crit}}$  above which the ADAF branch disappears ( $\dot{M}_{\text{crit}} \sim 0.1\dot{M}_{\text{Edd}}$  when  $\alpha_B = 0.05$ ). The maximum luminosity of the disk staying in the ADAF branch is only 10 % of the Eddington luminosity. To explain the observed X-ray hard state with luminosity as high as 20% of the Eddington luminosity, the disk should be kept in optically thin state. Such disks can exist when  $\zeta \gtrsim 0.5$  in our models, where  $\zeta$  is the parameter which parameterizes the radial variation of the advection rate of the toroidal magnetic flux.

We also obtained steady global transonic solutions including magnetic fields and obtained  $\Sigma - \dot{M}$  relation. When  $\zeta \sim 0$ , we could not obtain solutions above certain critical accretion rate. The reason simply comes from the fact that we chose the ADAF-like outer boundary condition. This means that there exists no solution connecting from such outer boundary to inner region with weak magnetic field. When  $\zeta \sim 1$ , we can obtain solutions for larger  $\dot{M}$ . These solutions consist of four regions, the outer boundary region, the outer transition region, the inner low- $\beta$  region and the inner ADAF region.

In this paper, we assumed single temperature plasma and included only the bremsstrahlung cooling. In magnetized accretion disks, electrons will also be cooled by synchrotron radiation and inverse Compton effects. These processes will increase the luminosity of the disk and decrease the critical accretion rate for the transition to the low- $\beta$  disk. In optically thin, hot accretion disks, since the gas temperature becomes so high while electrons are cooled by radiation, the electron temperature can become lower than the ion temperature. Such two-temperature accretion disk models were studied by Shapiro, Lightman, Eardley (1976) and Ichimaru (1977). Nakamura et al. (1997) obtained transonic solutions of two temperature accretion disks including synchrotron cooling and inverse Compton effects. However, plasma  $\beta$  was assumed to be uniform in their paper. In subsequent papers, we would like to obtain solutions of magnetized two temperature disks subjecting to the cooling instability.

The authors thank Drs. M.A. Abramowicz, C. Akizuki, C. Done, J. Fukue, S. Hirose, Y. Kato, S. Mineshige, K. Ohsuga, R.A. Remillard, K. Watarai, and S. Miyaji for their valuable comments and discussions. Part of this work was carried out when R.M. and M.M. attended the KITP program on "Physics of Astrophysical Outflows and Accretion Disks" at UCSB. This work was supported in part by the Grants-in-Aid for Scientific Research of the Ministry of Education, Culture, Sports, Science and Technology (RM: 17030003), Japan Society for the Promotion of Science (JSPS) Research Fellowships for Young Scientists (MM: 17-1907, 18-1907), and by the National Science Foundation under Grant No. PHY99-07949.

## References

Abramowicz, M. A., Chen, X., Kato, S., Lasota, J. P. & Regev, O. 1995, ApJ, 438, L37  
 Balbus, S. A. & Hawley, J. F. 1991, ApJ, 376, 214  
 Begelman, M. C. & Pringle, J. E. 2006, astro-ph/0612300  
 Brandenburg, A., Nordlund, A., Stein, R. F. & Torkelsson, U. 1995, ApJ, 446, 741  
 Done, C. & Gierliński, M. 2003, MNRAS, 342, 1041  
 Eardley, D. M., Lightman, A. P. & Shapiro, S. L. 1975, ApJ, 199, L153  
 Gierliński, M. & Newton, J. 2006, MNRAS, 370, 837  
 Hawley, J. F., Gammie, C. F. & Balbus, S. A. 1995, ApJ, 440, 742  
 Hawley, J. F., Gammie, C. F. & Balbus, S. A. 1996, ApJ, 464, 690  
 Hawley, J. F. 2000, ApJ, 528, 462  
 Hawley, J. F. & Krolik, J. H. 2001, ApJ, 548, 348  
 Hawley, J. F. & Krolik, J. H. 2002, ApJ, 566, 164  
 Hirose, S., Krolik, J. H. & Stone, J. M. 2006, ApJ, 640, 901  
 Ichimaru, S. 1977, ApJ, 214, 840  
 Kato, S., Fukue, J. & Mineshige, S. 1998, BLACK-HOLE ACCRETION DISKS (Kyoto: Kyoto University Press)  
 Machida, M., Hayashi, M. R. & Matsumoto, R. 2000, ApJ, 532, L67  
 Machida, M. & Matsumoto, R. 2003, ApJ, 585, 429  
 Machida, M., Nakamura, K. E. & Matsumoto, R. 2004, PASJ, 56, 671  
 Machida, M., Nakamura, K. E. & Matsumoto, R. 2006, PASJ, 58, 193  
 Matsumoto, R., Kato, S., Fukue, J. & Okazaki, A. T. 1984, PASJ, 36, 71  
 Matsumoto, R. & Tajima, T. 1995, ApJ, 445, 767  
 Matsumoto, R., 1999, NUMERICAL ASTROPHYSICS, ed. S. M. Miyama, T. Tomisaka & T. Hanawa (Amsterdam: Kluwer Academic Publishers) 195  
 Miller, K. A. & Stone, J. M. 2000, ApJ, 534, 398  
 Mineshige, S., Kusunose, M. & Matsumoto, R. 1995, ApJ, 445, L43  
 Nakamura, K. E., Kusunose, M. Matsumoto, R., & Kato, S. 1997, PASJ, 49, 503  
 Narayan, R. & Yi, I. 1994, ApJ, 428, L13  
 Narayan, R. & Yi, I. 1995, ApJ, 452, 710  
 Paczynsky, B. & Wiita, P. J. 1980, A&A, 88, 23  
 Pariev, V. I., Blackman, E. G. & Boldyrev, S. A. 2003, A&A, 407, 403  
 Parker, E. N. 1966, ApJ, 145, 811  
 Pessah, M. E., & Psaltis, D. 2005, ApJ, 628, 879  
 Pessah, M. E., Chan, C. & Psaltis, D. 2006, astro-ph/0610565  
 Sano, T. & Inustuka, S. 2001, ApJ, 605, L179  
 Sano, T., Inustuka, S., Turner, N. J. & Stone, J. M. 2004, ApJ, 605, 321  
 Shakura, N. I. & Sunyaev, R. A. 1973, A&A, 24, 337  
 Shapiro, S. L., Lightman, A. P. & Eardley, D. M. 1976, ApJ, 204, 187  
 Shibata, K., Tajima, T. & Matsumoto, R. 1990, ApJ, 350, 295  
 Shibasaki, N. & Hoshi, R. 1975, Progress of Theoretical Physics, 54, 706  
 Thorne, K. S., Price, R. H. 1975, ApJ, 195, L101

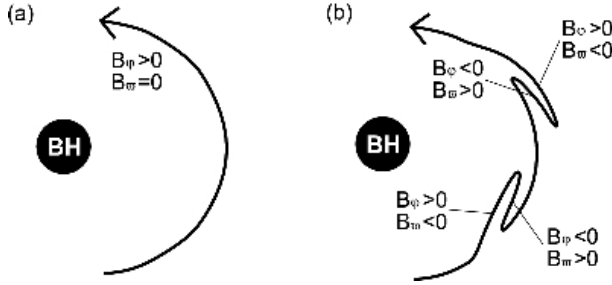


**Fig. 1.** A schematic picture of a magnetic field line inside the accretion disk. (a) Axisymmetric disk threaded by mean azimuthal magnetic fields. (b) Turbulent disk with mean azimuthal magnetic fields and fluctuating magnetic fields. The azimuthal average of the radial component of the magnetic field,  $\langle B_\varpi \rangle$ , is small because positive and negative  $B_\varpi$  cancel out. On the other hand, the azimuthal average of the product of the radial and toroidal component,  $\langle B_\varpi B_\varphi \rangle$ , has a large negative value because  $B_\varpi B_\varphi$  does not change sign when magnetic fields are deformed by nonlinear growth of MRI.

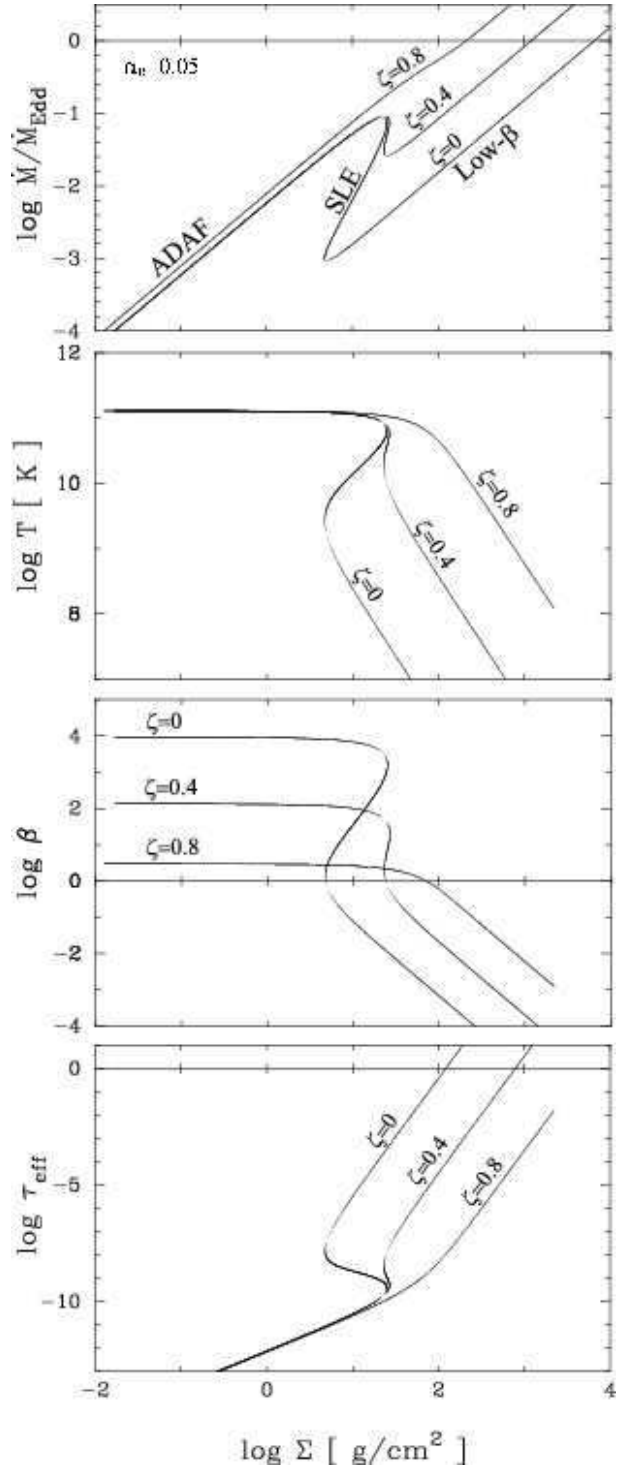


**Fig. 2.** Local thermal equilibrium curves of accretion disks at  $\varpi = 5r_s$  on the  $\Sigma - \dot{M}$ ,  $\Sigma - T$ ,  $\Sigma - \beta$ ,  $\Sigma - \tau_{\text{eff}}$  plane for optically thin accretion disks with  $M = 10M_\odot$ ,  $\alpha_B = 0.05$  and  $\zeta = 0, 0.4, 0.8$ . SLE indicates the cooling dominated branch by Shapiro, Lightman, Eardley (1976).  $\dot{M}_{\text{Edd}} = 4\pi GM/(\eta_e \kappa_{\text{esc}} c)$  is the Eddington accretion rate where the energy conversion efficiency  $\eta_e$  is taken to be  $\eta_e = 0.1$ .

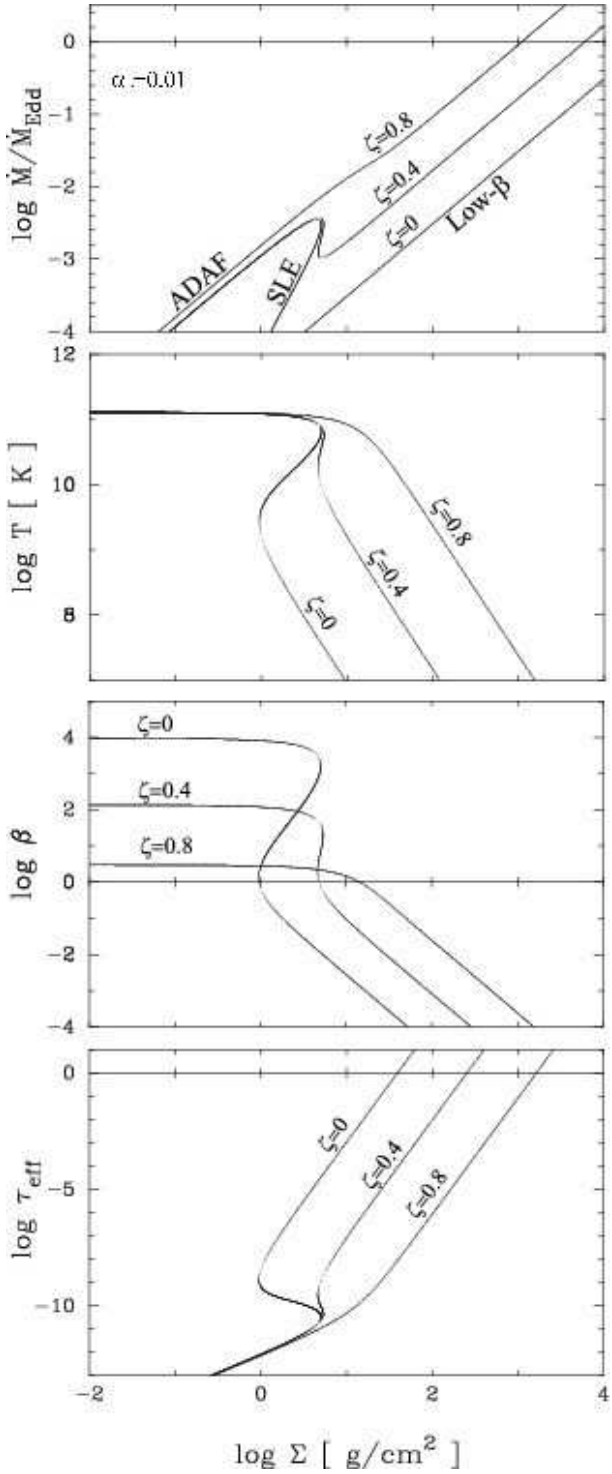


Fig. 3. Same as figure 2 but for  $\alpha_B = 0.01$ .

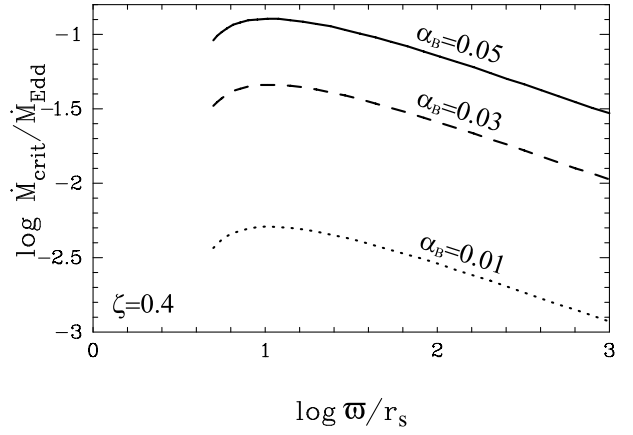
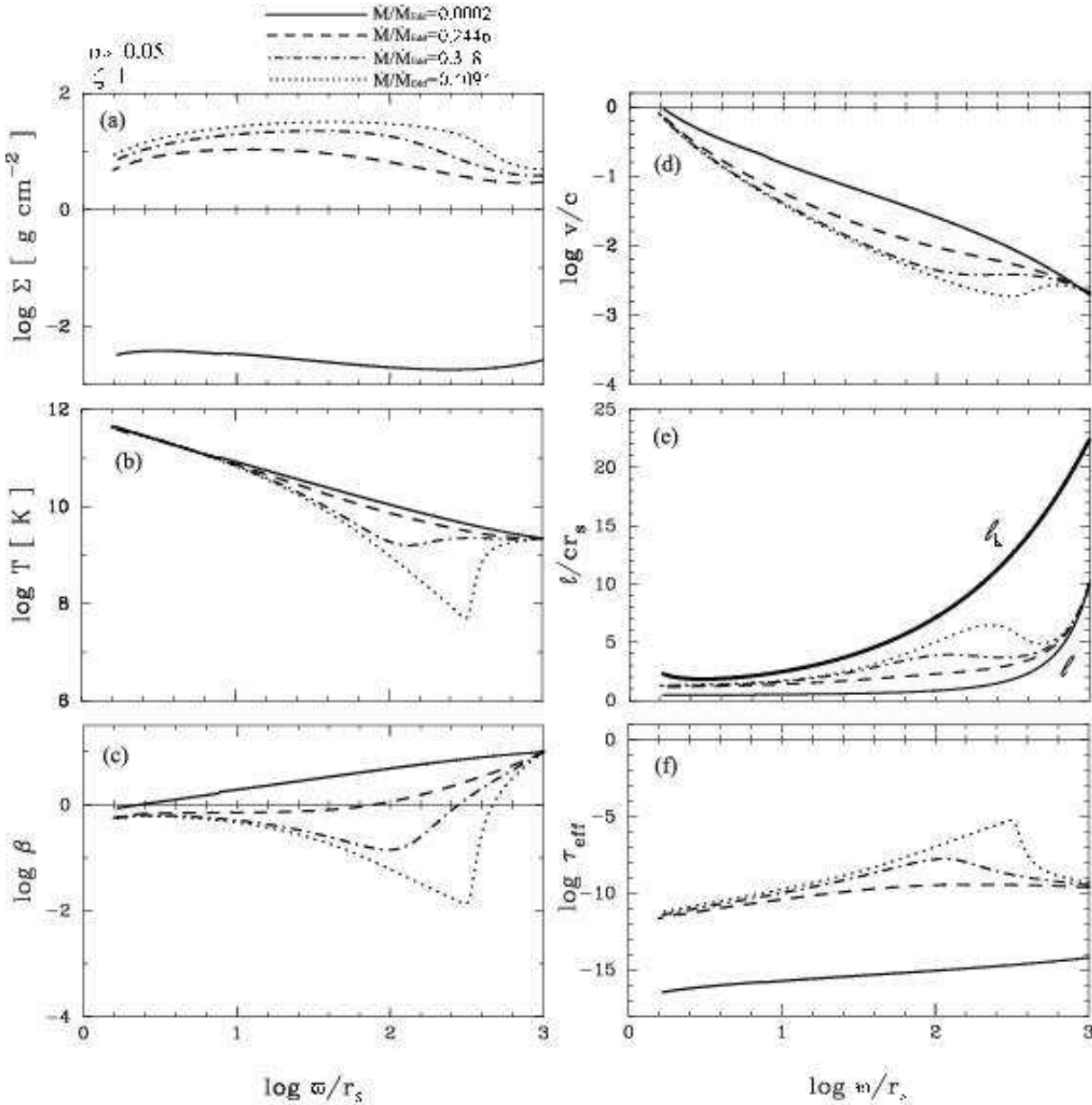
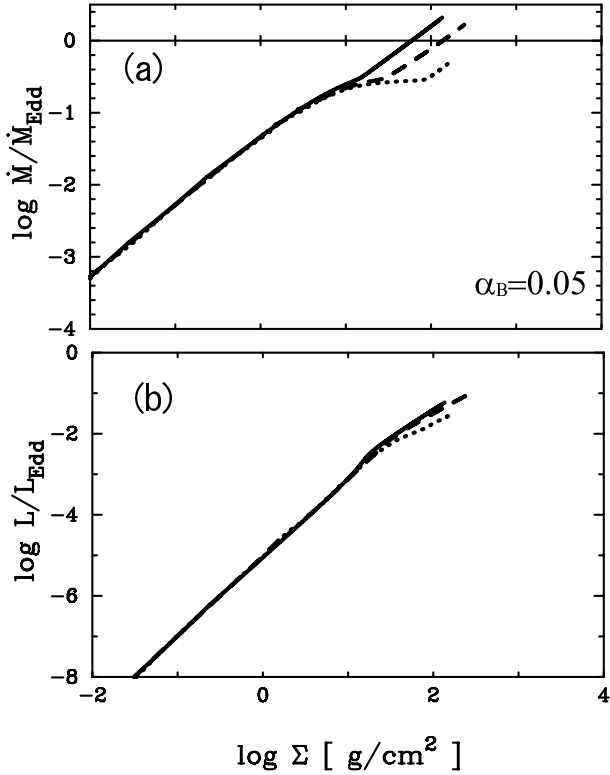


Fig. 4. The radial dependence of  $\dot{M}_{\text{crit}}$  for  $\zeta = 0.4$  and  $\alpha_B = 0.05$  (solid),  $0.03$  (dashed) and  $0.01$  (dotted).



**Fig. 5.** The radial structure of the disk when  $\zeta = 1$  and  $\dot{M}/\dot{M}_{\text{Edd}} = 0.0002$  (solid),  $0.2446$  (dashed),  $0.3181$  (dashed-dotted), and  $0.4094$  (dotted) with  $\alpha_B = 0.05$ . Thick solid curve in panel (e) shows the Keplerian angular momentum distribution.



**Fig. 6.** (a)  $\Sigma - \dot{M}$  relation at  $5r_s$  obtained by global solutions with  $\alpha_B = 0.05$  when  $\zeta = 1$  (solid), 0.8 (dashed), and 0.6 (dotted). (b) The relation between  $\Sigma$  and luminosity  $L/L_{\text{Edd}}$ .